Intraseasonal Precipitation Variability over West Africa under 1.5 °C and 2.0 °C Global Warming Scenarios: Results from CORDEX RCMs

Obed M. Ogega [1,2], **Benjamin A. Gyampoh** [3] **and Malcolm N. Mistry** [4,5,*]

[1] School of Environmental Studies, Kenyatta University, 43844-00100 Nairobi, Kenya; o.ogega@aasciences.africa

[2] Programmes, the African Academy of Sciences, 24916-00502 Nairobi, Kenya

[3] Fisheries and Watershed Management, Kwame Nkrumah University of Science and Technology, PMB, KNUST, Kumasi, Ghana; bagyampoh@knust.edu.gh

[4] Department of Economics, Ca' Foscari University of Venice, 30121 Venice, Italy

[5] Centro Euro-Mediterraneo sui Cambiamenti Climatici (CMCC), 30175 Venice, Italy

[*] Correspondence: malcolm.mistry@unive.it

Abstract: This study assessed the performance of 24 simulations, from five regional climate models (RCMs) participating in the Coordinated Regional Climate Downscaling Experiment (CORDEX), in representing spatiotemporal characteristics of precipitation over West Africa, compared to observations. The top five performing RCM simulations were used to assess future precipitation changes over West Africa, under 1.5 °C and 2.0 °C global warming levels (GWLs), following the representative concentration pathway (RCP) 8.5. The performance evaluation and future change assessment were done using a set of seven 'descriptors' of West African precipitation namely the simple precipitation intensity index (SDII), the consecutive wet days (CWD), the number of wet days index (R1MM), the number of wet days with moderate and heavy intensity precipitation (R10MM and R30MM, respectively), and annual and June to September daily mean precipitation (ANN and JJAS, respectively). The performance assessment and future change outlook were done for the CORDEX–Africa subdomains of north West Africa (WA-N), south West Africa (WA-S), and a combination of the two subdomains. While the performance of RCM runs was descriptor- and subregion- specific, five model runs emerged as top performers in representing precipitation characteristics over both WA-N and WA-S. The five model runs are CCLM4 forced by ICHEC-EC-EARTH (r12i1p1), RCA4 forced by CCCma-CanESM2 (r1i1p1), RACMO22T forced by MOHC-HadGEM2-ES (r1i1p1), and the ensemble means of simulations made by CCLM4 and RACMO22T. All precipitation descriptors recorded a reduction under the two warming levels, except the SDII which recorded an increase. Unlike the WA-N that showed less frequency and more intense precipitation, the WA-S showed increased frequency and intensity. Given the potential impact that these projected changes may have on West Africa's socioeconomic activities, adjustments in investment may be required to take advantage of (and enhance system resilience against damage that may result from) the potential changes in precipitation.

Keywords: ensembles; regional and mesoscale modelling; climate; tropics; seasonal prediction; intraseasonal rainfall variability; CORDEX; West African monsoon

1. Introduction

West Africa's climate is influenced by several factors including altitude, proximity to the tropical Atlantic Ocean, migration of the Inter-Tropical Convergence Zone (ITCZ), and the location of dominant atmospheric high- and low-pressure systems [1]. The region's main rainy season occurs between April and September in coincidence with the northerly migration of the Inter-Tropical Convergence Zone (ITCZ). Towards the coast, countries like Ghana and Côte d'Ivoire experience bi-modal rainfall with the main (minor) rainy season being April to July (September to October). In between these rainy seasons are dry periods, mainly from November to March. Temperatures across the region are relatively high throughout the year ranging from around 21 to 30 °C. The highest temperatures are experienced in the Sahara Desert, north of the region, where average maximum temperatures regularly exceed 40 °C.

The Sahel and tropical West Africa have long been identified as hotspots of climate change [2] under the representative concentration pathways (RCP) 4.5 and 8.5 [3]. Some projections [4] show a possibility of unprecedented climate events occurring over West Africa as early as the late 2030s to early 2040s. Several studies have also estimated temperatures over West Africa to range between 3 and 6 °C above the late 20th century baseline by the end of the 21st century [5–7].

Using regional climate models (RCMs) participating in the Coordinated Regional Climate Downscaling Experiment (CORDEX), Mounkaila et al.[8] established that CCRM5, RCA35, REMO, RegCM3, and WRF simulate rainfall onset dates over West Africa fairly well. The assessment used RCMs forced by the European Centre for Medium-Range Weather Forecasts (ECMWF) Interim Re-Analysis (ERAINT) [9]. More recently, Diaconescu et al. [10] inferred that two CORDEX–Africa RCMs (CanRCM4 and CRCM5, forced by ERAINT) could adequately reproduce large-scale features of the West Africa Monsoon (WAM) precipitation albeit with less accuracy over the northern rainy bands.

Several other studies [11–13] have made similar CORDEX–Africa RCM assessments using RCMs driven by ERAINT. For example, Akinsanola et al. [14,15] found the Rossby Centre Regional Climate Model–RCA4 driven by select general circulation models (GCMs) to replicate the historical rainfall characteristics over West Africa. However, most of the works done over the study domain have either focused on ERAINT-forced CORDEX RCMs or only used a small ensemble of CORDEX RCM simulations. Given that projections are generated using RCMs forced by GCMs and not reanalysis data, the use of model performance assessment done using RCMs forced by re-analysis data to evaluate future changes in the climate system can be misleading [16].

The availability of GCMs from the sixth phase of the Coupled Model Intercomparison Project (CMIP6) [17] provides an opportunity for more accurate climate assessments. Ajibola et al. [18] established that while a set of high-resolution models CMIP6 GCMs could adequately reproduce precipitation over West Africa, biases were recorded especially for extreme events. The biases result from, among others, relatively coarser spatial resolutions that fail to adequately resolve local features (e.g., orography) compared to RCMs [19]. Currently, efforts such as CORDEX 2 [20] are ongoing towards availability of sufficient RCM downscaled datasets from CMIP6 GCMs. Our study complements earlier works by assessing outputs from a large multi-model ensemble (24 simulations) from CORDEX RCMs, forced by CMIP5 GCMs. Specifically, we first assess the performance of five RCMs forced by 10 GCMs (24 runs) in reproducing West Africa's historical precipitation characteristics relative to observations. The top-performing model runs are then used to assess future precipitation changes under the 1.5 °C and 2.0 °C global warming levels (GWL1.5 and GWL2.0, respectively), using climate projections under the RCP 8.5 scenario. The rest of the paper is organized into Materials and Methods (2), Results (3), Discussion (4), and Conclusions (5).
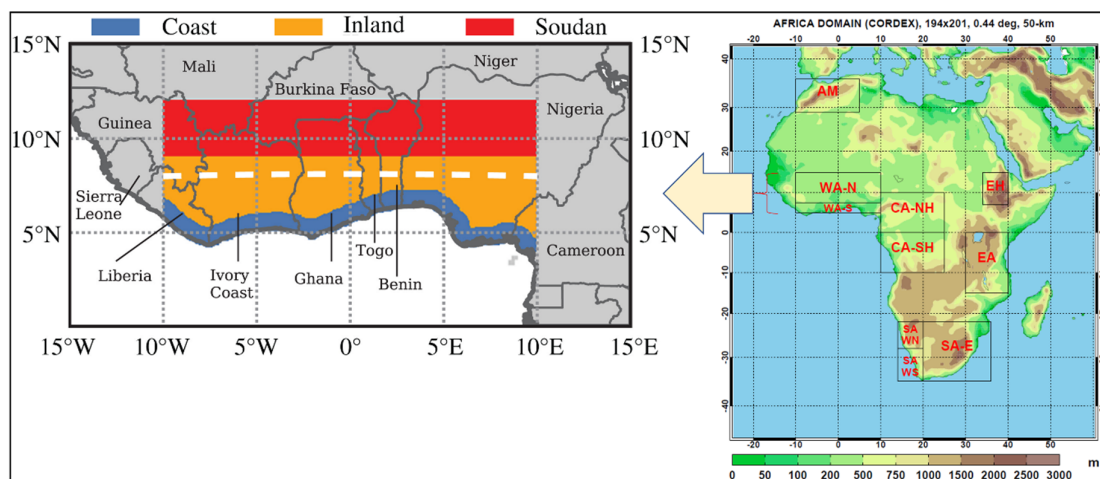
2. Materials and Methods

2.1. Study Region

West Africa lies between longitude 20° W and 20° E and latitude 0° and 20° N. The region covers an area of 8 million square kilometres and 16 countries over the southern portion of the bulge of the African continent, which extends westward to the Atlantic Ocean. It covers approximately 25% of Africa, with a broad range of ecosystems, bioclimatic regions, and habitats ranging from rain forest to desert. The Sahara Desert and the Niger River (Africa's third-longest river) are the main physical features of the region [1].

West Africa's climate ranges from arid and desert conditions in the north (close to the Sahara Desert) to humid tropical monsoon conditions along the coast (to the south). Annual precipitation mainly follows a latitudinal gradient with less than 400 mm/year in the Northern Sahel and more than 1500 mm/year along the coast of the Gulf of Guinea [21]. The dry/wet season over West Africa lengthens/decreases with increasing latitude.

Our study focused on two CORDEX–Africa subdomains of West Africa namely north West Africa (WA-N) and south West Africa (WA-S) based on the general characterisation of their climatic features [22–24]. As detailed in Figure 1, WA-S ranges from around 5 to 7.5° N, and is characterized by a sub-humid climate with mean annual precipitation ranging from 1250 to 1500 mm. WA-N combines the Savannah zone and part of the Sahel (ranging from about 8–15° N), and is characterized by annual mean rainfall ranging from 750 to 1250 mm.

Figure 1. Map of Coordinated Regional climate Downscaling Experiment (CORDEX) West Africa domains (marked WA-N and WA-S) where the analysis was done. Map adapted from https://bit.ly/2BR3qBJ and [25] under the terms of the Creative Commons Attribution 4.0 International license (CC-BY 4.0).

2.2. Data

2.2.1. RCM Data

Total daily near-surface precipitation data from 24 CORDEX–Africa RCM realisations (bias un-corrected and in native form) resulting from single or multiple ensemble runs (Table 1) were used in this study. The RCMs, described in detail by [26], were forced by CMIP5 GCMs, and have a spatial resolution of about 50 km at the equator [27]. Our study focused on realisations under RCP 8.5 given that it provides the largest set of ensemble members compared to other RCPs. Further, RCP 8.5 represents the most realistic warming scenario considering today's global greenhouse gas emission trajectory [28] and has been widely used for analysis of projections in sub-Saharan Africa [14,29–31].

Table 1. List of regional climate models (RCMs) used in our study (data accessed in March 2020 from http://bit.ly/2RoIist).

Institute	RCM	Ensemble	Driving Model
Climate Limited-Area Modelling (CLM) Community	CLMcom COSMOCLM (CCLM4)	r1i1p1	MOHC-HadGEM2-ES
			MPI-M-MPI-ESM-LR
			CNRM-CERFACS-CNRM-CM5
		r12i1p1	ICHEC-EC-EARTH
Max Planck Institute (MPI), Germany	MPI-CSC-REMO2009 (REMO2009)	r12i1p1	ICHEC-EC-EARTH
		r1i1p1	MPI-M-MPI-ESM-LR
Sveriges Meteorologiska och Hydrologiska Institut (SMHI), Sweden	SMHI Rossby Centre Regional Atmospheric Model (RCA4)	r1i1p1	CSIRO-QCCCE-CSIRO-Mk3-6-0
			MIROC-MIROC5
			MOHC-HadGEM2-ES
			NCC-NorESM1-M
			MPI-M-MPI-ESM-LR
			IPSL-IPSL-CM5A-MR
			NOAA-GFDL-GFDL-ESM2M
			CCCma-CanESM2
			CNRM-CERFACS-CNRM-CM5
			ICHEC-EC-EARTH
		r12i1p1	ICHEC-EC-EARTH
		r2i1p1	MPI-M-MPI-ESM-LR
		r3i1p1	MPI-M-MPI-ESM-LR
			ICHEC-EC-EARTH
Koninklijk Nederlands Meteorologisch Instituut (KNMI), Netherlands	KNMI Regional Atmospheric Climate Model, version 2.2 (RACMO22T)	r1i1p1	MOHC-HadGEM2-ES
			ICHEC-EC-EARTH
Danish Meteorological Institute (DMI)	DMI-HIRHAM5 (HIRHAM5)	r3i1p1	ICHEC-EC-EARTH
		r1i1p1	NCC-NorESM1-M

2.2.2. Observational Data

The daily Climate Hazards Group InfraRed Precipitation with Station data (CHIRPS), version 2.0 [32] for the period 1983–2005 was used as the reference observational precipitation data. The CHIRPS dataset ranges from 1981 to near present and integrates satellite imagery (0.05° resolution) with in situ station data producing a gridded rainfall timeseries. To facilitate comparison, the Tropical Applications of Meteorology using Satellite and ground-based observations, version 3 (TAMSAT3) [33] was used as a second reference dataset for precipitation. TAMSAT3 is daily rainfall dataset based on high-resolution thermal-infrared observations and available from 1983 to the near-present. It is based on the disaggregation of 5-day total TAMSAT rainfall estimates to a daily time-step using daily cold cloud duration. In so doing, the dataset provides a temporally consistent historic and near-real time daily rainfall information for all of Africa. We also considered the daily version of the Global Precipitation Climatology Project dataset (GPCP-Daily). GPCP-Daily is based on the monthly version and produced by optimally merging precipitation estimates from infrared, microwave, and sounder data observed by the international constellation of precipitation-related satellites, and precipitation gauge analyses [34]. However, GPCP-Daily is only available from October 1996 to present, making it too short (9 years) for our baseline (1976–2005). CHIRPS and TAMSAT3 provide 25 and 23 years of analysis, respectively, and have been validated and used widely in studies on West African precipitation [33,35,36].

Computations were done on the native data grids [37], before bilinearly interpolating [38] the processed files to make it possible to compare observations and models. Additionally, computations were done for each year before averaging to get the climatology of descriptors for the periods of interest to minimize the risk posed by simple averaging [39,40].

2.3. Data Analysis

This study was done in two parts: (1) evaluating the performance of 24 CORDEX–Africa RCM realisations in reproducing West Africa's historical intra-seasonal precipitation characteristics and (2) estimating future precipitation change projections over the study domain using the top-performing model runs. The choice of top-performing model runs was informed by, in part, the existence of a large set of model runs produced by a growing number of models with differing characteristics and notable interdependence [41]. For instance, the skill of representing observed climate and trends differs from one model to another [42,43]. Using a large group of model simulations can be impracticable and pose a risk of bias given that the performance of models is strongly dependent on the scale and variable being investigated [44]. Additionally, several studies have shown that a large multi-model ensemble performs dismally, compared to an ensemble of few top-performing models in the group [41,45–47].

Nonetheless, our choice of a few more-adequate models was not intended to discredit the performance of the other models. We appreciate the potential risk of biased or overconfident results especially if the number of models is small [48]. However, the risk is minimized when a robust method of model performance assessment is used. In this study, we used nine model runs from a pool of 24 simulations, to estimate future precipitation changes over the study domain.

Specifically, we evaluated the performance of RCM runs based on their skill in reproducing spatial and temporal patterns of West African precipitation (hereinafter 'descriptors'). The descriptors (Table 2) represent three categories of daily precipitation indices defined by the Expert Team on Climate Change Detection and Indices (ETCCDI) [49]. The three categories are (i) the mean and strong intensity indices; (ii) occurrence indices; and (iii) duration indices, herein represented by (a) simple precipitation intensity index (SDII); (b) R1mm, R10mm, and R30mm; and (c) CWD, respectively. The indices have been widely used to study precipitation over West Africa [10,50] and beyond [47,51,52]. The other two descriptors are the annual (ANN) and seasonal (JJAS) daily mean precipitation.

Performance evaluation was done using simulations from five CORDEX–Africa RCMs forced by GCMs. The period 1983 to 2005 was chosen to correspond to data availability for reference data (CHIRPS and TAMSAT3) available from 1981 and 1983 to the near present, respectively. It also corresponds to historical simulations of the CORDEX–Africa RCMs (up to year 2005). The performance assessment was done in three tiers for a better representation of the study domain. Here, the 24 model runs were evaluated on their ability to represent precipitation characteristics over WA-S, WA-N, and a combination of WA-S and WA-N.

The performance of the RCM runs in reproducing the spatial patterns for all the precipitation descriptors, relative to observations, was done using spatial correlation coefficients (PCC). The temporal part was assessed using an inter-annual variability skill score (IVS) [45], defined as follows:

$$\text{IVS} = \left(\frac{\sigma_m}{\sigma_o} - \frac{\sigma_o}{\sigma_m} \right)^2 \tag{1}$$

where σ_o and σ_m represent the standard deviation for observations and models, respectively. An IVS value of 0 implies that σ_o is equal to σ_m, and the closer an IVS value is to 0, the better its skill in simulating the inter-annual variability [45].

The model performance assessment was done using detrended data to minimize the risk of potentially spurious variable relations [53]. To rank the performance of model runs based on the two criteria (temporal and spatial precipitation characteristics), a comprehensive rating index MR [46]; was used, as follows:

$$\text{MR} = 1 - \frac{1}{nm} \sum_{i=1}^{n} rank_i \tag{2}$$

where *n* is the number of descriptors and *m* the number of RCM runs. The model with an MR value closest to 1 gives the best skill of simulation, compared to other models under consideration [46].

Table 2. Climate indices and precipitation statistics used as descriptors of a precipitation over West Africa.

Descriptor	Acronym	Description	Unit
Simple precipitation intensity index	SDII	Mean precipitation amount on a wet day. Let RR_{ij} be the daily precipitation amount on wet day w ($RR \geq 1$ mm) in period *j*. If *W* represents the number of wet days in *j* then the simple precipitation intensity index $SDII_j = \text{sum} (RR_{wj})/W$	mm/day
Number of wet days index	R1mm	Defined as the number of days with precipitation ≥ 1 mm/day	Days
Number of wet days with moderate intensity precipitation	R10mm	Defined as the number of days with precipitation ≥ 10 mm/day and representing moderate intensity precipitation days	Days
Number of wet days with heavy intensity precipitation	R30mm	Defined as the number of days with precipitation ≥ 30 mm/day and representing heavy intensity precipitation days	Days
Consecutive wet days	CWD	Maximum length of wet spell, maximum number of consecutive days with $RR \geq 1$ mm: Let RR_{ij} be the daily precipitation amount on day *I* in period *j*. Count the largest number of consecutive days where: $RR_{ij} \geq 1$ mm	Days
Mean annual daily precipitation	ANN	For every adjacent sequence $t\_1, ..., t\_n$ of timesteps of the same year it is: $o(t, x) = mean\{i(t', x), t_1 < t' \leq t_n\}$; computed for January-December of every year in the series	mm/day
Mean daily precipitation for JJAS season	JJAS	For every adjacent sequence $t\_1, ..., t\_n$ of timesteps of the same year it is: $o(t, x) = mean\{i(t', x), t_1 < t' \leq t_n\}$; computed for June-September of every year in the series	mm/day

Results from model ranking (MR) based on IVS and PCC, for the three sub-domains, were plotted in scatter diagrams to facilitate comparison. Here, two sets of MR values were calculated. The first set used PCC values where the model run with the highest correlation coefficient was ranked first, while the one with the lowest coefficient was ranked last. Given that the performance of model runs was ranked against seven descriptors, model run 'X' can be ranked number 1 for descriptor 1 and number 5 for descriptor 2, etc. Hence, a formula (Equation (2)) was used to rank the overall performance of individual model runs in all the seven categories (descriptors). The second set of MR values used model runs that were ranked based on their performance in reproducing year-to-year precipitation characteristics (IVS; Equation (1)). Here, the model run with the lowest IVS was ranked

first while the model run with the highest IVS was ranked last. The MR equation was then used to give the overall ranking based on IVS. Lastly, MR values based on PCC were plotted against MR values based on IVS. The top-performing models (relatively) are found in the 1st quadrant (Q1), while the least performing models are found in the Q3 of the scatter plot. Other studies that have used this method include [46,47].

The top-performing model runs for each sub-domain were used to compute future precipitation changes for all the descriptors using projections under the RCP 8.5 scenario. A detailed analysis conducted by [54] identified (using a subset of GCM simulations driving CORDEX–Africa RCMs) years 2022 and 2037 as mid-years for 30-year windows, when GWL1.5 and GWL2.0, respectively, are likely to be first experienced. Their analysis was done with reference to the period 1861–1890 as the pre-industrial period. Our study adapted these mid-years and computed future changes in precipitation over West Africa by subtracting precipitation climatology values in the period 1976–2005 (hereinafter CTL) from the precipitation climatology values in periods 2008–2037, 2023–2052, and 2071–2100, corresponding to GWL1.5, GWL2.0, future (FUT), respectively, under RCP 8.5. The future changes were computed for all the seven descriptors.

3. Results

3.1. RCM Performance Assessment

Scatter plots (Figures S1 to S6 in the Supplementary Materials) for model run rankings based on correlation coefficients (PCCs) and interannual variability scores (IVS) were made, to show the performance of the model runs. A summary of the top-performing model simulations in reproducing spatial and temporal precipitation characteristics over WA-N is shown in Table 3. Here, the top five simulations (agreed upon by both TAMSAT3 and CHIRPS) were CCLM4 forced by MOHC-HadGEM2-ES (r1i1p1), RCA4 forced by NCC-NorESM1-M (r1i1p1), IPSL-IPSL-CM5A-MR (r1i1p1), and ICHEC-EC-EARTH (r12i1p1), and an ensemble mean for model runs produced by RACMO22T.

Table 3. Top RCM runs per criteria for north West Africa (WA-N).

Reference dataset	Criterion	RCM	Driving GCM
CHIRPS	PCCs	RCA4	CNRM-CERFACS-CNRM-CM5 (r1i1p1), MPI-M-MPI-ESM-LR (r2i1p1), ICHEC-EC-EARTH (r3i1p1)
		REMO2009	Ensemble mean
		HIRHAM5	Ensemble mean
	IVS	RCA4	NCC-NorESM1-M (r1i1p1), CCCma-CanESM2 (r1i1p1), ICHEC-EC-EARTH (r3i1p1)
		RACMO22T	MOHC-HadGEM2-ES (r1i1p1)
		HIRHAM5	Ensemble mean
	Both PCCs and IVS	CCLM4	MOHC-HadGEM2-ES (r1i1p1)
		RCA4	NCC-NorESM1-M (r1i1p1), IPSL-IPSL-CM5A-MR (r1i1p1), CNRM-CERFACS-CNRM-CM5 (r1i1p1), ICHEC-EC-EARTH (r12i1p1), ICHEC-EC-EARTH (r3i1p1)
		CCLM4	Ensemble mean
		RACMO22T	Ensemble mean

Table 3. *Conts.*

Reference dataset	Criterion	RCM	Driving GCM
TAMSAT3	PCCs	RCA4	CSIRO-QCCCE-CSIRO-Mk3-6-0 (r1i1p1), NCC-NorESM1-M (r1i1p1), IPSL-IPSL-CM5A-MR (r1i1p1), CNRM-CERFACS-CNRM-CM5 (r1i1p1), ICHEC-EC-EARTH (r1i1p1)
	IVS	RCA4	CCCma-CanESM2 (r1i1p1),
		CCLM4	MOHC-HadGEM2-ES (r1i1p1), ICHEC-EC-EARTH (r12i1p1), Ensemble mean
		RACMO22T	MOHC-HadGEM2-ES (r1i1p1)
	Both PCCs and IVS	CCLM4	MOHC-HadGEM2-ES (r1i1p1),
		RCA4	MPI-M-MPI-ESM-LR (r1i1p1), IPSL-IPSL-CM5A-MR (r1i1p1), NCC-NorESM1-M (r1i1p1), CCCma-CanESM2 (r1i1p1), ICHEC-EC-EARTH (r12i1p1), MPI-M-MPI-ESM-LR (r3i1p1)
		RACMO22T	Ensemble mean

For the WA-S region (Table 4), CCLM4 forced by MPI-M-MPI-ESM-LR (r1i1p1) and ICHEC-EC-EARTH (r12i1p1), RACMO22T forced by MOHC-HadGEM2-ES (r1i1p1), HIRHAM5 forced by ICHEC-EC-EARTH (r3i1p1), and an ensemble mean for simulations produced by RACMO22T emerged as the top-performing model runs.

Additionally, the performance of model simulations in reproducing spatial and temporal precipitation characteristics at both WA-S and WA-N was ranked (Table 5). Here, the model runs agreed upon by both reference data sets (TAMSAT3 and CHIRPS) were CCLM4 forced by ICHEC-EC-EARTH (r12i1p1), RCA4 forced by CCCma-CanESM2 (r1i1p1), RACMO22T forced by MOHC-HadGEM2-ES (r1i1p1), an ensemble mean for simulations done by CCLM4, and an ensemble mean for simulations done by RACMO22T.

With CHIRPS as the reference dataset, RCA4 driven by CCCma-CanESM2 (r1i1p1) and RACMO22T driven by MOHC-HadGEM2-ES (r1i1p1) were the only simulations featuring among the top five performers in reproducing spatial precipitation characteristics for WA-N, WA-S, and both WA-N and WA-S regions. RCA4 driven by CNRM-CERFACS-CNRM-CM5 (r1i1p1) was the only RCM simulation featuring among the top five performers in reproducing interannual precipitation characteristics for WA-N, WA-S, and both WA-N and WA-S regions. Considering the performance of simulations in reproducing both spatial and temporal precipitation characteristics (compared to CHIRPS), none of the model runs featured among the top five performers in all three categories (WA-N, WA-S, and both WA-N and WA-S).

In the case of TAMSAT3 as the reference dataset, no model simulation was featured among the top five performers in reproducing interannual precipitation characteristics in all three categories (WA-N, WA-S, and both WA-N and WA-S). CCLM4 and RACMO22T driven by MOHC-HadGEM2-ES (r1i1p1) and an ensemble mean of model runs driving the CCLM4 featured among the top five performers in reproducing the spatial precipitation characteristics in all three categories.

Overall, five model runs emerged as top performers in reproducing precipitation characteristics (both spatial and temporal) at both WA-N and WA-S, with reference to both TAMSAT3 and CHIRPS. The five model runs were CCLM4 forced by ICHEC-EC-EARTH (r12i1p1), RCA4 forced by CCCma-CanESM2 (r1i1p1), RACMO22T forced by MOHC-HadGEM2-ES (r1i1p1), and the ensemble means of simulations done by CCLM4 and RACMO22T. Assessing the performance of four CORDEX RCMs in reproducing

climate characteristics over southern Ghana, Ashaley et al. [55] identified the RCA4 model forced by CCCma-CanESM2 as one of the top-performing models. Our results agree with this finding and add value by providing a list of additional top-performing model runs (and for a bigger domain) over West Africa.

Table 4. As in Table 3 but for south West Africa (WA-S).

Reference dataset	Criterion	RCM	Driving GCM
CHIRPS	PCCs	RCA4	CNRM-CERFACS-CNRM-CM5 (r1i1p1), CCCma-CanESM2 (r1i1p1), MPI-M-MPI-ESM-LR (r3i1p1),
		RACMO22T	MOHC-HadGEM2-ES (r1i1p1)
		HIRHAM5	ICHEC-EC-EARTH (r3i1p1)
	IVS	RCA4	CCCma-CanESM2 (r1i1p1)
		RACMO22T	MOHC-HadGEM2-ES (r1i1p1)
		CCLM4	MPI-M-MPI-ESM-LR (r1i1p1), ICHEC-EC-EARTH (r12i1p1), Ensemble mean
	Both PCCs and IVS	CCLM4	MPI-M-MPI-ESM-LR (r1i1p1), ICHEC-EC-EARTH (r12i1p1)
		RCA4	CCCma-CanESM2 (r1i1p1), ICHEC-EC-EARTH (r3i1p1),
		RACMO22T	MOHC-HadGEM2-ES (r1i1p1), Ensemble mean
		HIRHAM5	ICHEC-EC-EARTH (r3i1p1), Ensemble mean
TAMSAT3	PCCs	RCA4	MOHC-HadGEM2-ES (r1i1p1), MPI-M-MPI-ESM-LR (r2i1p1)
		HIRHAM5	ICHEC-EC-EARTH (r3i1p1), NCC-NorESM1-M (r1i1p1)
		CCLM4	CNRM-CERFACS-CNRM-CM5 (r1i1p1)
	IVS	CCLM4	MOHC-HadGEM2-ES (r1i1p1), Ensemble mean
		RCA4	MOHC-HadGEM2-ES (r1i1p1)
		RACMO22T	MOHC-HadGEM2-ES (r1i1p1), Ensemble mean
	Both PCCs and IVS	CCLM4	MOHC-HadGEM2-ES (r1i1p1), ICHEC-EC-EARTH (r12i1p1), MPI-M-MPI-ESM-LR (r1i1p1)
		RCA4	MOHC-HadGEM2-ES (r1i1p1),
		HIRHAM5	ICHEC-EC-EARTH (r3i1p1), NCC-NorESM1-M (r1i1p1), Ensemble mean
		RACMO22T	MOHC-HadGEM2-ES (r1i1p1),

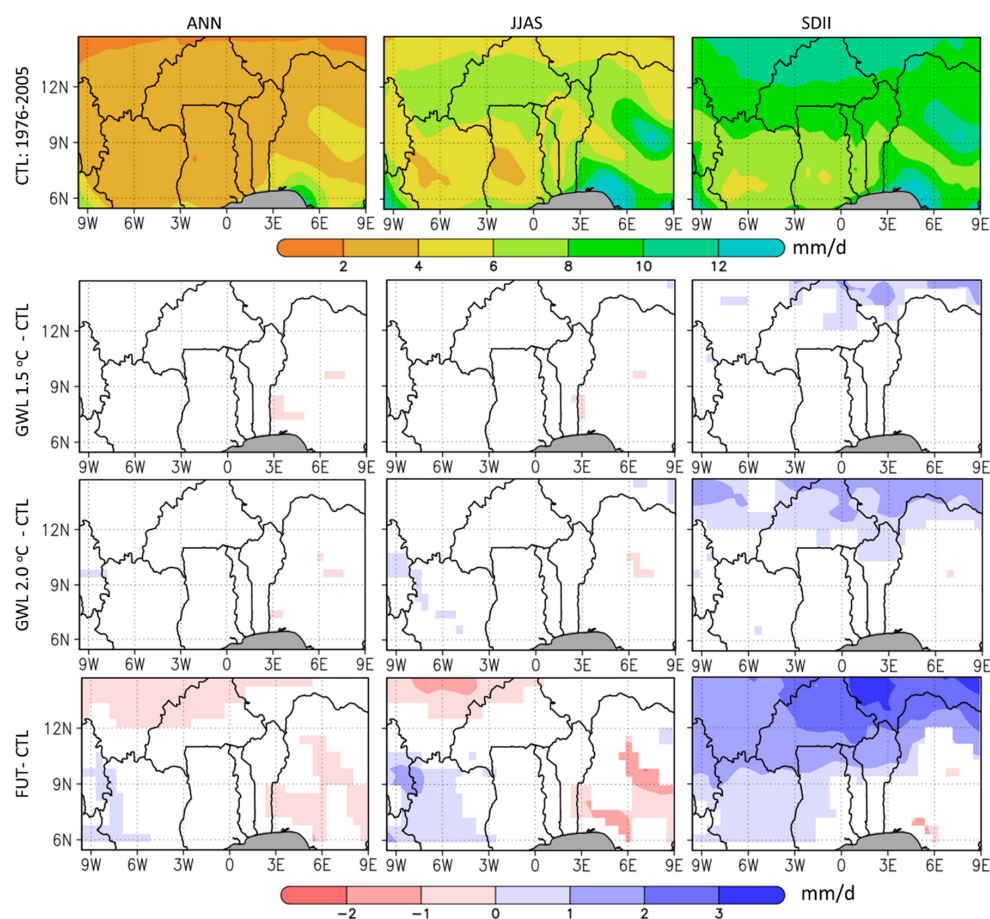**Table 5.** As in Table 3 but combining the performance of model runs at both WA-N and WA-S.

Reference dataset	Criterion	RCM	Driving GCM
CHIRPS	PCCs	RCA4	CNRM-CERFACS-CNRM-CM5 (r1i1p1), MPI-M-MPI-ESM-LR (r2i1p1), ICHEC-EC-EARTH (r3i1p1),
		HIRHAM5	ICHEC-EC-EARTH (r3i1p1), Ensemble mean
	IVS	RCA4	CCCma-CanESM2 (r1i1p1), ICHEC-EC-EARTH (r3i1p1),
		RACMO22T	MOHC-HadGEM2-ES (r1i1p1),
		CCLM4	ICHEC-EC-EARTH (r12i1p1), Ensemble mean
	Both PCCs and IVS	CCLM4	ICHEC-EC-EARTH (r12i1p1), Ensemble mean
		RCA4	NCC-NorESM1-M (r1i1p1), CCCma-CanESM2 (r1i1p1), ICHEC-EC-EARTH (r3i1p1),
		RACMO22T	MOHC-HadGEM2-ES (r1i1p1), Ensemble mean
		HIRHAM5	ICHEC-EC-EARTH (r3i1p1)
TAMSAT3	PCCs	RCA4	CSIRO-QCCCE-CSIRO-Mk3-6-0 (r1i1p1), MOHC-HadGEM2-ES (r1i1p1), IPSL-IPSL-CM5A-MR (r1i1p1), CNRM-CERFACS-CNRM-CM5 (r1i1p1), MPI-M-MPI-ESM-LR (r2i1p1)
	IVS	CCLM4	ICHEC-EC-EARTH (r12i1p1), MOHC-HadGEM2-ES (r1i1p1), Ensemble mean
		RCA4	CCCma-CanESM2 (r1i1p1)
		RACMO22T	MOHC-HadGEM2-ES (r1i1p1)
	Both PCCs and IVS	CCLM4	MOHC-HadGEM2-ES (r1i1p1), MPI-M-MPI-ESM-LR (r1i1p1), ICHEC-EC-EARTH (r12i1p1), Ensemble mean
		RCA4	CCCma-CanESM2 (r1i1p1)
		HIRHAM5	Ensemble mean
		RACMO22T	MOHC-HadGEM2-ES (r1i1p1), Ensemble mean

Notably, the performance of model runs was location- and descriptor-specific. No single model run emerged best in reproducing all the seven descriptors—hence the need for a model ranking formula (Equation (2)). The relatively inconsistent performance of model simulations in reproducing the set precipitation descriptors from one region and criteria to another could be, partly, as a result of the predominantly convective nature of precipitation over the study domain [25,56]. The convective precipitation occurs in the mesoscale which begins at around 5 km—significantly lower than CORDEX-Africa RCMs' resolutions of about 50 km at the equator. Consequently, the relatively coarse resolutions of models make it difficult for them to adequately resolve the convective precipitation systems over the study domain [25,57]. Some of the mesoscale convective systems that affect West Africa include squall-lines [58], organized convective systems [59], and mesoscale convective systems [59,60].
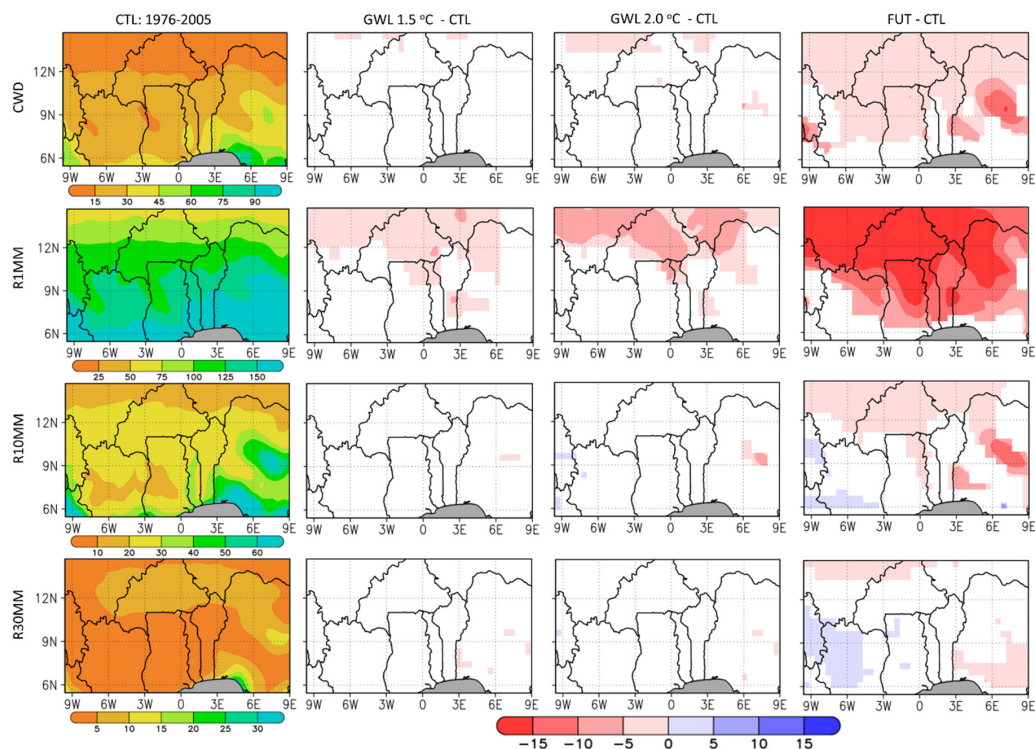
3.2. Future Precipitation Changes over West Africa

Using a multi-model ensemble mean of the top-performing model runs determined in Section 3.1, projected changes in the spatial climatology of all seven precipitation descriptors for West Africa were plotted (Figures 2 and 3). During the control period (CTL; 1976–2005), daily mean annual precipitation ranging from about 2 mm at the north of the study domain to about 9 mm at the south was recorded. The JJAS season recorded precipitation ranging from about 4 mm to about 12 mm per day with the highest amount recorded over central (around 7.5 E, 9.1 N) and southern Nigeria (about 3–9.2 E, 5.8–6.2 N). Most of the study domain recorded a simple daily precipitation intensity index of between 8 and 12 mm. The highest intensity (exceeding 12 mm) was recorded over central and southern Nigeria.

Under the GWL1.5, no major significant changes in mean daily precipitation at the annual (ANN) and seasonal (JJAS) were recorded over the study domain. Where recorded, precipitation seemed to reduce by about 1 mm/day for both ANN and JJAS. A GWL2.0 was likely to introduce minor (about 1 mm/day) wet and dry biases at a few places over the study domain. An increase of between 1 and 2 mm/day was recorded for the simple daily precipitation index (SDII) over some parts north of the study domain. The SDII seemed to intensify under GWL2.0. Although the changes under GWL2.0 were more than changes under GWL1.5, most of the study domain recorded no significant changes for ANN, JJAS, and SDII.

Figure 2. Future precipitation changes for ANN, JJAS, and SDII (at 95% confidence level) for GWL1.5, GWL2.0, and future (FUT) relative to the control period (CTL), under the RCP 8.5 scenario. Areas with no significant changes are shown in white while water bodies are shown in grey.

Figure 3. As in Figure 2 but for CWD, R1MM, R10MM, and R30MM. All units are in days/year.

Projections (under RCP 8.5) showed a reduction in daily mean precipitation of up to 2 mm in several areas to the north and east of the study domain for ANN and JJAS, by the end of the 21st century. However, an increase of up to 2 mm in mean daily precipitation for ANN and JJAS was recorded over areas south-west of the study domain. Most of the study domain recorded an increase in SDII by the end of the 21st century. The increase was more pronounced to the north of the domain with changes exceeding 3 mm/day recorded in some areas. No significant changes were recorded over most of Nigeria and southern Togo and Benin (south-east of the study domain). A few areas south-west of Nigeria recorded a decrease in SDII of up to 2 mm.

Our findings on ANN, JJAS, and SDII are consistent with similar works done in the study domain. Evaluating the impacts of GWL1.5 and GWL2.0 over Senegal, Mbaye et al. [61] established a possible marginal decrease in annual and July–September mean precipitation. Their study also pointed to the possibility of a slight increase in heavy precipitation events over Senegal under the two global warming levels for the RCP 8.5 scenario. Looking at Africa in general, Nikulin et al. [54] reported a tendency towards wetter conditions in annual average precipitation over central and eastern Sahel, but with a low model agreement. There seems to be a consensus (consistent with our findings) that the daily precipitation intensity is likely to increase under a global warming scenario [54,61,62].

Looking at the descriptors that show the frequency of precipitation aspects (Figure 3), consecutive wet days (CWD) over the domain seemed to reduce with latitude with about 15 days/annum at the north and 75 days south of the study region. Minor significant changes (about -5 days) were recorded over a few areas under GWL1.5 and GWL2.0. By the end of the 21st century, most of the study domain recorded a reduction in CWD of between 5 and 15 days/annum. Areas in central Nigeria recorded the largest reduction (about 15 days/annum), while areas south of the study domain recorded no significant changes.

An average of about 50 rainy days (R1MM) were recorded in the north of the study domain and at least 150 days/annum in the south. Most of the domain recorded between 10 and 30 days of wet days with moderate intensity precipitation (R10MM). For wet days with heavy intensity precipitation (R30MM), most of the domain recorded less than 15 days/annum. No major significant changes were recorded over the domain for R1MM, R10MM, and R30MM, save for a slight reduction of up to
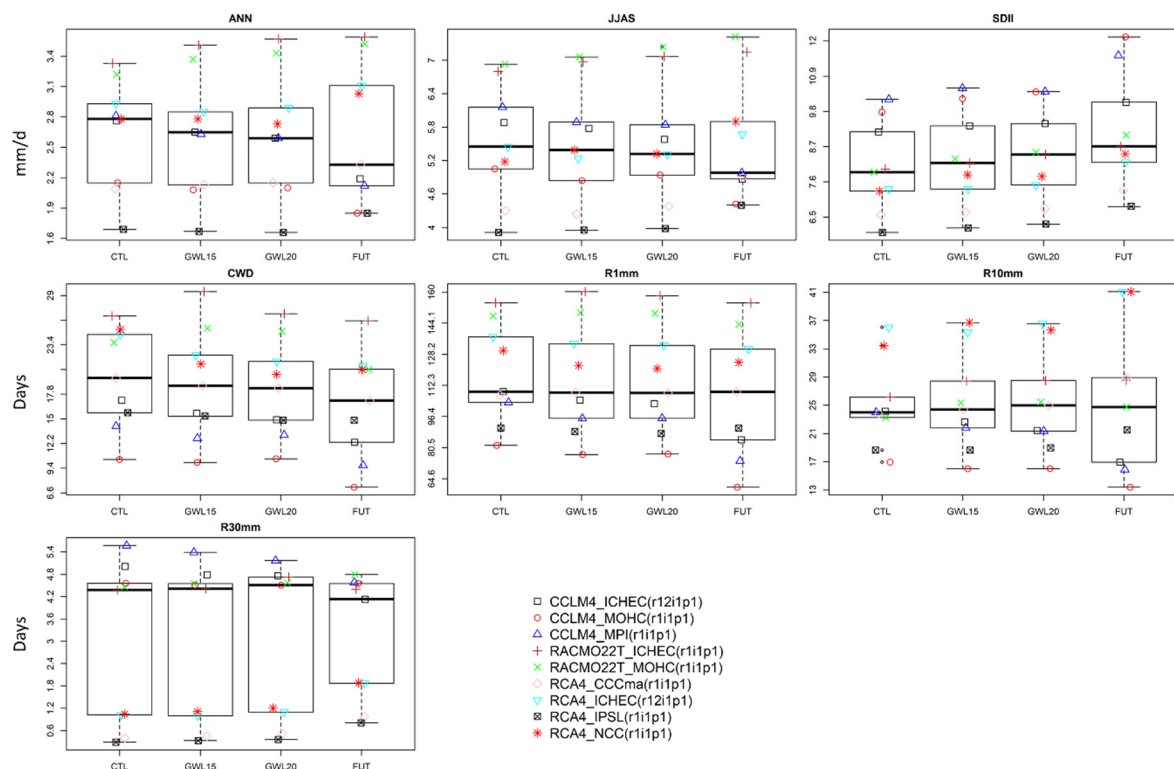
10 days/annum, especially for R1MM over some areas north of the domain. Over the future (FUT) period, the greatest change (exceeding 15 days/annum in most of the domain) was expected for R1MM. R10MM and R30MM recorded a slight reduction of about 5 days/annum in many parts of the domain except the south-west where an increase of about 5 days/annum was recorded.

Overall, the 1.5 °C and 2.0 °C global warming levels did not show significant effect on precipitation over many parts of the study domain. Specifically, all precipitation descriptors recorded a reduction under the two warming scenarios except SDII which recorded an increase. The northern part of the study domain recorded most changes compared to the south. Considering the future period (FUT, 2071–2100), SDII and R1MM recorded the greatest change, with many areas exceeding 2 mm/day and -15 days/annum, respectively. A few areas to the south-west of the domain recorded more episodes of wet bias than the rest of the study domain.

To enhance the understanding of future precipitation changes over the north and south subdomains of our study area, boxplots were done using a set of nine top-performing model simulations determined in Section 3.1. The boxplots showed the spread of the nine CORDEX RCM runs in reproducing the seven precipitation descriptors over the two subdomains as detailed in the following subsections.

3.2.1. Future Precipitation Changes over the WA-N Sub-Region

First, precipitation changes over the northern part of the study domain (WA-N) were assessed (Figure 4). Here, the spread of model runs was greatest (relatively) for R30MM, implying a lower model agreement compared to other precipitation descriptors. Compared to the control period (CTL), no noticeable changes were recorded for R1MM and R30MM under GWL1.5. A slight decrease (increase) was recorded for Annual, JJAS, and CWD (SDII and R10MM).

Figure 4. Future precipitation changes over the WA-N region under GWL15, GWL20, and FUT, respectively, compared to the 1976–2005 control period (CTL). Boxplots were plotted using top-performing model runs determined in Section 3.1, using climate projections under the RCP 8.5 scenario.

　　　　Under GWL2.0, a further reduction (increase) in annual, JJAS, and CWD (R30MM, R10MM, and SDII) was recorded. No conspicuous changes were recorded for R1MM. Under the future scenario (FUT), discernible negative (positive) changes were recorded for annual, JJAS, R30MM, and CWD (SDII). No major changes were recorded for R1MM and R10MM. As in the spatial plots, the boxplots showed a reducing trend in annual mean daily precipitation (ANN) and CWD, but an increasing trend in SDII. This implies a potential for a decreasing frequency and increasing intensity of precipitation over the WA-N region.

3.2.2. Future Precipitation Changes over the WA-S Sub-Region

　　　　Secondly, an analysis of future change projections over the southern part of the study domain (WA-S; Figure 5) was done. Unlike the case of WA-N, where a decreasing trend was observed, WA-S showed an increasing trend for ANN and JJAS from the GWL1.5 to FUT scenarios. SDII showed an increasing trend while R30MM, which showed no remarkable change over WA-N, showed an increase in the three scenarios relative to the CTL.

　　　　Except for ANN, JJAS, and SDII, the difference between the impact of GWL1.5 and GWL2.0 on precipitation over WA-S was minimal. Changes during the FUT period were more pronounced for all the descriptors compared to GWL1.5 and GWL2.0. All but two descriptors (CWD and R1MM) showed a positive change during the FUT period than the CTL period. Overall, unlike the WA-N, where less frequent but more intense precipitation was recorded, the WA-S showed potential for more frequent and intense precipitation under the three scenarios.

Figure 5. As in Figure 4 but for WA-S region.

4. Discussion

Our findings agree with similar studies that have shown the possibility of enhanced precipitation over West Africa in the future [63] and add value by (i) delineating the expected future changes in two sub-domains of West Africa; and (ii) assessing more precipitation characteristics for a better representation of West African precipitation. For instance, we show that the number of wet days with heavy intensity precipitation (R30MM) is projected to increase (remain unchanged) over WA-S (WA-N) under GWL1.5, GWL2.0, and FUT. Our results also show a reduction in consecutive wet days for both WA-N and WA-S with the reduction over WA-S being more pronounced. These results qualify earlier studies that alluded to the possibility of extreme rainfall events [64], increased precipitation intensity [65,66], and increased dry spells [67] over the study domain.

Over 75% of West Africa's population lives in areas that have been affected at least once in every two years by flood, dust/sandstorm, and drought in the last three decades alone [68]. This comes with great impacts on livelihoods and requires holistic planning and strategies that incorporate different scenarios and early warning development mechanisms. Yet, many countries in West Africa lack adequate meteorological and hydrological capacity to collect, process, and disseminate climate information for early warning to vulnerable communities [68]. Therefore, the results of this study provide useful information to support decision making and investments in water resources management, agriculture, and energy—the most affected sectors of the West African economy.

Our study corroborates previous works that inferred a possibility of more floods and crop water stress over the study domain [69]. Additionally, we show that the southern part of West Africa (WA-S) will potentially experience more intense and frequent precipitation compared to the northern part (WA-N), which records potential for less frequent and more intense precipitation. As West Africa experiences rapid population increase, rapid demographic and socioeconomic transformations, urbanization, and rising incomes, greater stress is placed on food systems. Hence, tough decisions will have to be made to minimize greenhouse gas emissions and adapt agricultural systems in preparation for possible future precipitation changes. The possibility of a drying climate calls for common but differentiated climate change adaptation strategies to address current and future national, regional, and transboundary challenges in the study domain.

As a caveat, our study relied on a study done by [54] to determine periods corresponding to the 1.5 °C and 2.0 °C global warming levels. Further, our study focused on a subset of GCMs participating in CORDEX. Various sub-sets of GCMs and the choice of the reference pre-industrial period may give varying estimates of the future period when the 1.5 °C and 2.0 °C global warming levels are likely to be reached. Hence, we recommend further research to explore various scenarios and enhance the understanding of the impacts of global warming levels on climate systems. Additionally, a large ensemble of climate projections can introduce bias especially when ensembles consist of models with similar components or from the same family [42]. A common issue with CORDEX simulations is that not all RCMs downscale all GCMs. For instance, the RCA4 model contributed 14 out of the 24 simulations considered in our study. The sparse RCM-GCM matrix can potentially introduce a bias towards specific RCMs and hence, potentially lead to overconfidence on future climate change scenarios. Our study does not address these limitations and only provides insights aimed at spurring further research and discussions on future climate changes over the study domain.

5. Conclusions

Through a relatively low model agreement, this study confirmed the difficulty of climate models (at the current spatial resolutions) to represent West African precipitation adequately due to, in part, mesoscale climate systems [25,57,58]. The performance of the 24 model simulations was descriptor and subdomain specific with no single model run featuring as a top performer in representing the spatial and temporal characteristics of all the seven precipitation descriptors, across all the three sub-domain categories. Nonetheless, five model runs emerged as top performers namely CCLM4 forced by ICHEC-EC-EARTH (r12i1p1), RCA4 forced by CCCma-CanESM2 (r1i1p1),

RACMO22T forced by MOHC-HadGEM2-ES (r1i1p1), and the ensemble means of simulations done by CCLM4 and RACMO22T. Assessment of potential future precipitation changes under 1.5 °C and 2.0 °C global warming levels under the RCP 8.5 scenario showed a minimal impact on West African precipitation, relative to the 1976–2005 control period (CTL). All precipitation descriptors recorded a reduction under the two warming levels, except SDII, which recorded an increase. Unlike the WA-N, which showed less frequent and more intense precipitation, the WA-S showed an increase in frequency and intensity. These changes seemed to be more robust in the future period (2071–2100) under the RCP 8.5 scenario.

Given the potentially significant impact these projected changes may have on West Africa's socioeconomic activities, adjustments in investment may be required to take advantage of the heavier and more intense precipitation for enhanced productivity and water availability. The potential decrease in the number of rainy days and the consecutive wet days call for investment in water harvesting initiatives to ensure water availability for domestic and agricultural use during the dry periods. The potential for more heavy and intense precipitation events poses a risk to infrastructure over the study domain, which is vulnerable to floods [70,71].

References

1. Daron, J.D. Regional Climate Messages for West Africa. In *Climate System Analysis Group (CSAG)*; University of Cape Town: Cape Town, South Africa, 2014; Available online: https://bit.ly/3geaCHu (accessed on 12 October 2020).

2. Diffenbaugh, N.S.; Giorgi, F. Climate change hotspots in the CMIP5 global climate model ensemble. *Clim. Chang.* **2012**, *114*, 813–822. [CrossRef] [PubMed]

3. Moss, R.H.; Edmonds, J.A.; Hibbard, K.A.; Manning, M.R.; Rose, S.K.; Van Vuuren, D.P.; Carter, T.R.; Emori, S.; Kainuma, M.; Kram, T.; et al. The next generation of scenarios for climate change research and assessment. *Nature* **2010**, *463*, 747–756. [CrossRef] [PubMed]

4. Mora, C.; Frazier, A.G.; Longman, R.J.; Dacks, R.S.; Walton, M.M.; Tong, E.J.; Sanchez, J.J.; Kaiser, L.R.; Stender, Y.O.; Anderson, J.M.; et al. The projected timing of climate departure from recent variability. *Nature* **2013**, *502*, 183–187. [CrossRef] [PubMed]

5. Meehl, G.A.; Covey, C.; Delworth, T.; Latif, M.; McAvaney, B.; Mitchell, J.F.B.; Stouffer, R.J.; Taylor, K.E. THE WCRP CMIP3 Multimodel Dataset: A New Era in Climate Change Research. *Bull. Am. Meteorol. Soc.* **2007**, *88*, 1383–1394. [CrossRef]

6.　Fontaine, B.; Roucou, P.; Monerie, P.-A. Changes in the African monsoon region at medium-term time horizon using 12 AR4 coupled models under the A1b emissions scenario. *Atmos. Sci. Lett.* **2011**, *12*, 83–88. [CrossRef]

7.　Monerie, P.-A.; Fontaine, B.; Roucou, P. Expected future changes in the African monsoon between 2030 and 2070 using some CMIP3 and CMIP5 models under a medium-low RCP scenario. *J. Geophys. Res. Atmos.* **2012**, *117*. [CrossRef]

8.　Mounkaila, M.S.; Abiodun, B.J.; Omotosho, J.B. Assessing the capability of CORDEX models in simulating onset of rainfall in West Africa. *Theor. Appl. Climatol.* **2014**, *119*, 255–272. [CrossRef]

9.　Dee, D.P.; Uppala, S.M.; Simmons, A.J.; Berrisford, P.; Poli, P.; Kobayashi, S.; Andrae, U.; Balmaseda, M.A.; Balsamo, G.; Bauer, P.; et al. The ERA-Interim reanalysis: Configuration and performance of the data assimilation system. *Q. J. R. Meteorol. Soc.* **2011**, *137*, 553–597. [CrossRef]

10.　Diaconescu, E.P.; Gachon, P.; Scinocca, J.; Laprise, R. Evaluation of daily precipitation statistics and monsoon onset/retreat over western Sahel in multiple data sets. *Clim. Dyn.* **2015**, *45*, 1325–1354. [CrossRef]

11.　Diallo, I.; Sylla, M.B.; Giorgi, F.; Gaye, A.T.; Camara, M. Multimodel GCM-RCM Ensemble-Based Projections of Temperature and Precipitation over West Africa for the Early 21st Century. *Int. J. Geophys.* **2012**, *2012*, 1–19. [CrossRef]

12.　Crétat, J.; Vizy, E.K.; Cook, K.H. The relationship between African easterly waves and daily rainfall over West Africa: Observations and regional climate simulations. *Clim. Dyn.* **2015**, *44*, 385–404. [CrossRef]

13.　Poan, E.D.; Gachon, P.; Dueymes, G.; Diaconescu, E.; Laprise, R.; Sanda, I.S. West African monsoon intraseasonal activity and its daily precipitation indices in regional climate models: Diagnostics and challenges. *Clim. Dyn.* **2016**, *47*, 3113–3140. [CrossRef]

14.　Akinsanola, A.; Ajayi, V.; Adejare, A.; Adeyeri, O.; Gbode, I.; Ogunjobi, K.; Nikulin, G.; Abolude, A. Evaluation of rainfall simulations over West Africa in dynamically downscaled CMIP5 global circulation models. *Theor. Appl. Climatol.* **2018**, *132*, 437–450. [CrossRef]

15.　Gnitou, G.T.; Ma, T.; Tan, G.; Ayugi, B.; Nooni, I.K.; Alabdulkarim, A.; Tian, Y. Evaluation of the Rossby Centre Regional Climate Model Rainfall Simulations over West Africa Using Large-Scale Spatial and Temporal Statistical Metrics. *Atmosphere* **2019**, *10*, 802. [CrossRef]

16.　Dosio, A.; Jones, R.G.; Jack, C.; Lennard, C.; Nikulin, G.; Hewitson, B. What can we know about future precipitation in Africa? Robustness, significance and added value of projections from a large ensemble of regional climate models. *Clim. Dyn.* **2019**, *53*, 5833–5858. [CrossRef]

17.　Eyring, V.; Bony, S.; Meehl, G.A.; Senior, C.A.; Stevens, B.; Stouffer, R.J.; Taylor, K.E. Overview of the Coupled Model Intercomparison Project Phase 6 (CMIP6) experimental design and organization. *Geosci. Model Dev.* **2016**, *9*, 1937–1958. [CrossRef]

18.　Ajibola, F.O.; Zhou, B.; Gnitou, G.T.; Onyejuruwa, A. Evaluation of the Performance of CMIP6 HighResMIP on West African Precipitation. *Atmosphere* **2020**, *11*, 1053. [CrossRef]

19.　Rummukainen, M. Added value in regional climate modeling. *Wiley Interdiscip. Rev. Clim. Chang.* **2016**, *7*, 145–159. [CrossRef]

20.　Gutowski, W.J., Jr.; Giorgi, F.; Timbal, B.; Frigon, A.; Jacob, D.; Kang, H.-S.; Raghavan, K.; Lee, B.; Lennard, C.; Nikulin, G.; et al. WCRP COordinated Regional Downscaling EXperiment (CORDEX): A diagnostic MIP for CMIP6. *Geosci. Model Dev.* **2016**, *9*, 4087–4095. [CrossRef]

21.　Froidurot, S.; Diedhiou, A. Characteristics of wet and dry spells in the West African monsoon system. *Atmospheric Sci. Lett.* **2017**, *18*, 125–131. [CrossRef]

22.　Omotosho, J.B.; Abiodun, B.J. A numerical study of moisture build-up and rainfall over West Africa. *Meteorol. Appl.* **2007**, *14*, 209–225. [CrossRef]

23.　Abiodun, B.J.; Adeyewa, Z.D.; Oguntunde, P.G.; Salami, A.T.; Ajayi, V.O. Modeling the impacts of reforestation on future climate in West Africa. *Theor. Appl. Climatol.* **2012**, *110*, 77–96. [CrossRef]

24.　Akinsanola, A.A.; Ogunjobi, K.O.; Gbode, I.E.; Ajayi, V.O. Assessing the Capabilities of Three Regional Climate Models over CORDEX Africa in Simulating West African Summer Monsoon Precipitation. *Adv. Meteorol.* **2015**, *2015*, 1–13. [CrossRef]

25.　Maranan, M.; Fink, A.H.; Knippertz, P. Rainfall types over southern West Africa: Objective identification, climatology and synoptic environment. *Q. J. R. Meteorol. Soc.* **2018**, *144*, 1628–1648. [CrossRef]

26. Nikulin, G.; Jones, C.; Giorgi, F.; Asrar, G.; Büchner, M.; Cerezo-Mota, R.; Christensen, O.B.; Déqué, M.; Fernandez, J.; Hänsler, A.; et al. Precipitation Climatology in an Ensemble of CORDEX-Africa Regional Climate Simulations. *J. Clim.* **2012**, *25*, 6057–6078. [CrossRef]

27. Meehl, G.A.; Moss, R.H.; Taylor, K.E.; Eyring, V.; Stouffer, R.J.; Bony, S.; Stevens, B. Climate Model Intercomparisons: Preparing for the Next Phase. *Eos Trans. Am. Geophys. Union* **2014**, *95*, 77–78. [CrossRef]

28. Taylor, K.E.; Stouffer, R.J.; Meehl, G.A. An Overview of CMIP5 and the Experiment Design. *Bull. Am. Meteorol. Soc.* **2012**, *93*, 485–498. [CrossRef]

29. Yan, Y.; Lu, R.; Li, C. Relationship between the Future Projections of Sahel Rainfall and the Simulation Biases of Present South Asian and Western North Pacific Rainfall in Summer. *J. Clim.* **2019**, *32*, 1327–1343. [CrossRef]

30. Gudoshava, M.; Misiani, H.O.; Segele, Z.T.; Jain, S.; Ouma, J.O.; Otieno, G.; Anyah, R.; Indasi, V.S.; Endris, H.S.; Osima, S.; et al. Projected effects of 1.5 °C and 2 °C global warming levels on the intra-seasonal rainfall characteristics over the Greater Horn of Africa. *Environ. Res. Lett.* **2020**, *15*, 034037. [CrossRef]

31. Ogega, O.M.; Alobo, M. Impact of 1.5 °C and 2 °C global warming scenarios on malaria transmission in East Africa. *AAS Open Res.* **2020**, *3*, 22. [CrossRef]

32. Funk, C.; Peterson, P.; Landsfeld, M.; Pedreros, D.; Verdin, J.; Shukla, S.; Husak, G.; Rowland, J.; Harrison, L.; Hoell, A.; et al. The climate hazards infrared precipitation with stations—A new environmental record for monitoring extremes. *Sci. Data* **2015**, *2*, 150066. [CrossRef] [PubMed]

33. Maidment, R.I.; Grimes, D.; Black, E.; Tarnavsky, E.; Young, M.; Greatrex, H.; Allan, R.P.; Stein, T.H.M.; Nkonde, E.; Senkunda, S.; et al. A new, long-term daily satellite-based rainfall dataset for operational monitoring in Africa. *Sci. Data* **2017**, *4*, 170063. [CrossRef] [PubMed]

34. Adler, R.F.; Huffman, G.J.; Chang, A.; Ferraro, R.; Xie, P.; Janowiak, J.; Rudolf, B.; Schneider, U.; Curtis, S.; Bolvin, B.; et al. The Version-2 Global Precipitation Climatology Project (GPCP) Monthly Precipitation Analysis (1979–Present). *J. Hydrometeorol.* **2003**, *4*, 1147–1167. [CrossRef]

35. Akinyemi, D.F.; Ayanlade, O.S.; Nwaezeigwe, J.O.; Ayanlade, A. A Comparison of the Accuracy of Multi-satellite Precipitation Estimation and Ground Meteorological Records Over Southwestern Nigeria. *Remote Sens. Earth Syst. Sci.* **2020**, *3*, 1–12. [CrossRef]

36. Harrison, L.; Funk, C.; Peterson, P. Identifying changing precipitation extremes in Sub-Saharan Africa with gauge and satellite products. *Environ. Res. Lett.* **2019**, *14*, 085007. [CrossRef]

37. Diaconescu, E.P.; Gachon, P.; Laprise, R. On the Remapping Procedure of Daily Precipitation Statistics and Indices Used in Regional Climate Model Evaluation. *J. Hydrometeorol.* **2015**, *16*, 2301–2310. [CrossRef]

38. Zhou, R.-G.; Hu, W.; Fan, P.; Ian, H. Quantum realisation of the bilinear interpolation method for NEQR. *Sci. Rep.* **2017**, *7*, 2511. [CrossRef]

39. Epstein, E.S. A Spectral Climatology. *J. Clim.* **1988**, *1*, 88–107. [CrossRef]

40. Narapusetty, B.; Delsole, T.; Tippett, M.K. Optimal Estimation of the Climatological Mean. *J. Clim.* **2009**, *22*, 4845–4859. [CrossRef]

41. Knutti, R.; Sedláček, J.; Sanderson, B.M.; Lorenz, R.; Fischer, E.M.; Eyring, V. A climate model projection weighting scheme accounting for performance and interdependence. *Geophys. Res. Lett.* **2017**, *44*, 1909–1918. [CrossRef]

42. Knutti, R.; Masson, D.; Gettelman, A. Climate model genealogy: Generation CMIP5 and how we got there. *Geophys. Res. Lett.* **2013**, *40*, 1194–1199. [CrossRef]

43. Reichler, T.; Kim, J. How Well Do Coupled Models Simulate Today's Climate? *Bull. Am. Meteorol. Soc.* **2008**, *89*, 303–312. [CrossRef]

44. Masson, D.; Knutti, R. Spatial-Scale Dependence of Climate Model Performance in the CMIP3 Ensemble. *J. Clim.* **2011**, *24*, 2680–2692. [CrossRef]

45. Chen, W.; Jiang, Z.; Li, L. Probabilistic Projections of Climate Change over China under the SRES A1B Scenario Using 28 AOGCMs. *J. Clim.* **2011**, *24*, 4741–4756. [CrossRef]

46. Jiang, Z.-H.; Li, W.; Xu, J.; Li, L. Extreme Precipitation Indices over China in CMIP5 Models. Part I: Model Evaluation. *J. Clim.* **2015**, *28*, 8603–8619. [CrossRef]

47. Ogega, O.M.; Koske, J.; Kung'u, J.B.; Scoccimarro, E.; Endris, H.S.; Mistry, M.N. Heavy precipitation events over East Africa in a changing climate: Results from CORDEX RCMs. *Clim. Dyn.* **2020**, *55*, 993–1009. [CrossRef]

48. Weigel, A.P.; Knutti, R.; Liniger, M.A.; Appenzeller, C. Risks of Model Weighting in Multimodel Climate Projections. *J. Clim.* **2010**, *23*, 4175–4191. [CrossRef]

49. Peterson, T.C.; Folland, C.; Gruza, G.; Hogg, W.; Plummer, N. *Report on the Activities of the Working Group on Climate Change Detection and Related Rapporteurs*; World Meteorological Organization (WMO): Geneva, Switzerland, 2001.

50. Dike, V.N.; Lin, Z.; Ibe, C.C. Intensification of Summer Rainfall Extremes over Nigeria during Recent Decades. *Atmosphere* **2020**, *11*, 1084. [CrossRef]

51. Osima, S.; Indasi, V.S.; Zaroug, M.; Endris, H.S.; Gudoshava, M.; Misiani, H.O.; Nimusiima, A.; Anyah, R.O.; Otieno, G.; Ogwang, B.A.; et al. Projected climate over the Greater Horn of Africa under 1.5 °C and 2 °C global warming. *Environ. Res. Lett.* **2018**, *13*, 065004. [CrossRef]

52. Bhatti, A.S.; Wang, G.; Ullah, W.; Ullah, S.; Hagan, D.F.T.; Nooni, I.K.; Lou, D.; Ullah, I. Trend in Extreme Precipitation Indices Based on Long Term In Situ Precipitation Records over Pakistan. *Water* **2020**, *12*, 797. [CrossRef]

53. Iler, A.M.; Inouye, D.W.; Schmidt, N.M.; Høye, T.T. Detrending phenological time series improves climate-phenology analyses and reveals evidence of plasticity. *Ecology* **2017**, *98*, 647–655. [CrossRef] [PubMed]

54. Nikulin, G.; Lennard, C.; Dosio, A.; Kjellström, E.; Chen, Y.; Hänsler, A.; Kupiainen, M.; Laprise, R.; Mariotti, L.; Maule, C.F.; et al. The effects of 1.5 and 2 degrees of global warming on Africa in the CORDEX ensemble. *Environ. Res. Lett.* **2018**, *13*, 065003. [CrossRef]

55. Ashaley, J.; Anornu, G.K.; Awotwi, A.; Gyamfi, C.; Anim-Gyampo, M. Performance evaluation of Africa CORDEX regional climate models: Case of Kpong irrigation scheme, Ghana. *Spat. Inf. Res.* **2020**, *28*, 735–753. [CrossRef]

56. Nicholson, S.E. The West African Sahel: A Review of Recent Studies on the Rainfall Regime and Its Interannual Variability. *ISRN Meteorol.* **2013**, *2013*, 1–32. [CrossRef]

57. Vogel, P.; Knippertz, P.; Fink, A.H.; Schlueter, A.; Gneiting, T. Skill of Global Raw and Postprocessed Ensemble Predictions of Rainfall over Northern Tropical Africa. *Weather Forecast.* **2018**, *33*, 369–388. [CrossRef]

58. Fink, A.H. Spatiotemporal variability of the relation between African Easterly Waves and West African Squall Lines in 1998 and 1999. *J. Geophys. Res. Atmos.* **2003**, *108*, 1–17. [CrossRef]

59. Mathon, V.; Laurent, H. Life cycle of Sahelian mesoscale convective cloud systems. *Q. J. R. Meteorol. Soc.* **2001**, *127*, 377–406. [CrossRef]

60. Laing, A.G.; Fritsch, J.M.; Negri, A.J. Contribution of Mesoscale Convective Complexes to Rainfall in Sahelian Africa: Estimates from Geostationary Infrared and Passive Microwave Data. *J. Appl. Meteorol.* **1999**, *38*, 957–964. [CrossRef]

61. Mbaye, M.L.; Sylla, M.B.; Tall, M. Impacts of 1.5 and 2.0 °C Global Warming on Water Balance Components over Senegal in West Africa. *Atmosphere* **2019**, *10*, 712. [CrossRef]

62. Weber, T.; Haensler, A.; Rechid, D.; Pfeifer, S.; Eggert, B.; Jacob, D. Analyzing Regional Climate Change in Africa in a 1.5, 2, and 3 °C Global Warming World. *Earth's Future* **2018**, *6*, 643–655. [CrossRef]

63. Dosio, A.; Turner, A.G.; Tamoffo, A.T.; Sylla, M.B.; Lennard, C.; Jones, R.G.; Terray, L.; Nikulin, G.; Hewitson, B. A tale of two futures: Contrasting scenarios of future precipitation for West Africa from an ensemble of regional climate models. *Environ. Res. Lett.* **2020**, *15*, 064007. [CrossRef]

64. Vizy, E.K.; Cook, K.H. Mid-Twenty-First-Century Changes in Extreme Events over Northern and Tropical Africa. *J. Clim.* **2012**, *25*, 5748–5767. [CrossRef]

65. Sylla, M.B.; Gaye, A.T.; Jenkins, G.S. On the Fine-Scale Topography Regulating Changes in Atmospheric Hydrological Cycle and Extreme Rainfall over West Africa in a Regional Climate Model Projections. *Int. J. Geophys.* **2012**, *2012*, 1–15. [CrossRef]

66. Haensler, A.; Saeed, F.; Jacob, D. Assessing the robustness of projected precipitation changes over central Africa on the basis of a multitude of global and regional climate projections. *Clim. Chang.* **2013**, *121*, 349–363. [CrossRef]

67. Salack, S.; Klein, C.; Giannini, A.; Sarr, B.; Worou, O.N.; Belko, N.; Bliefernicht, J.; Kunstman, H. Global warming induced hybrid rainy seasons in the Sahel. *Environ. Res. Lett.* **2016**, *11*, 104008. [CrossRef]

68. Economic Community of West African States. *Proceedings of the ECOWAS Hydromet Forum and Disaster Risk Reduction (DRR) Platform, Abuja, Nigeria, 19–21 September 2018*; Bamba, A., Banu, Z., Cheney, D., Dingel, C., Djuma, A., Fukuor, G., Ibrahim, M.S., Kablan, M.K.A., Koffi, K.V., Kouadio, K., Eds.; Economic Community of West African States (ECOWAS), Humanitarian and Social Affairs Directorate, ECOWAS Comission: Abuja, Nigeria, 2018; Available online: https://bit.ly/3g7Ldzi (accessed on 10 September 2020).

69. Deque, M.; Calmanti, S.; Christensen, O.B.; Dell'Aquila, A.; Maule, C.F.; Haensler, A.; Nikulin, G.; Teichmann, C. A multi-model climate response over tropical Africa at +2 °C. *Clim. Serv.* **2017**, *7*, 87–95. [CrossRef]

70. Zahiri, E.-P.; Bamba, I.; Famien, A.M.; Koffi, A.K.; Ochou, A.D. Mesoscale extreme rainfall events in West Africa: The cases of Niamey (Niger) and the Upper Ouémé Valley (Benin). *Weather Clim. Extrem.* **2016**, *13*, 15–34. [CrossRef]

71. Tazen, F.; Diarra, A.; Kabore, R.F.W.; Ibrahim, B.; Bologo/traoré, M.; Traoré, K.; Karambiri, H. Trends in flood events and their relationship to extreme rainfall in an urban area of Sahelian West Africa: The case study of Ouagadougou, Burkina Faso. *J. Flood Risk Manag.* **2019**, *12*, e12507. [CrossRef]